Available online at www.sciencedirect.com

ScienceDirect

Journal of Nuclear Materials 377 (2008) 72–79

journal of nuclear materials

www.elsevier.com/locate/jnucmat

Dose dependence of mechanical properties in tantalum and tantalum alloys after low temperature irradiation

Thak Sang Byun [a,*], Stuart A. Maloy [b]

[a] Oak Ridge National Laboratory, P.O. Box 2008, MS-6151, Oak Ridge, TN 37831, USA
[b] Los Alamos National Laboratory, MST-8, MS-H816, Los Alamos, NM 87545, USA

Abstract

The dose dependence of mechanical properties was investigated for tantalum and tantalum alloys after low temperature irradiation. Miniature tensile specimens of three pure tantalum metals, ISIS Ta, Aesar Ta1, Aesar Ta2, and one tantalum alloy, Ta–1W, were irradiated by neutrons in the high flux isotope reactor (HFIR) at ORNL to doses ranging from 0.00004 to 0.14 displacements per atom (dpa) in the temperature range 60–100 °C. Also, two tantalum–tungsten alloys, Ta–1W and Ta–10W, were irradiated by protons and spallation neutrons in the LANSCE facility at LANL to doses ranging from 0.7 to 7.5 dpa and from 0.7 to 25.2 dpa, respectively, in the temperature range 50–160 °C. Tensile tests were performed at room temperature and at 250 °C at nominal strain rates of about 10^{-3} s^{-1}. All neutron-irradiated materials underwent progressive irradiation hardening and loss of ductility with increasing dose. The ISIS Ta experienced embrittlement at 0.14 dpa, while the other metals retained significant necking ductility. Such a premature embrittlement in ISIS Ta is believed to be due to high initial oxygen concentrations picked up during a pre-irradiation anneal. The Ta–1W and Ta–10W specimens irradiated in spallation condition experienced prompt necking at yield since irradiation doses for those specimens were high ($\geqslant$0.7 dpa). At the highest dose, 25.2 dpa, the Ta–10W alloy specimen broke with little necking strain. Among the test materials, the Ta–1W alloy displayed the best combination of strength and ductility. The plastic instability stress and true fracture stress were nearly independent of dose. Increasing test temperature decreased strength and delayed the onset of necking at yield.
Published by Elsevier B.V.

1. Introduction

Tantalum and tantalum-based alloys are refractory metals that offer many favorable properties for nuclear and high temperature applications [1–8]. Their excellent ductility and high corrosion resistance make the metal very attractive for applications as structural materials [1]. Some high purity Ta metals have a total elongation of up to 50% at room temperature and retains significant ductility ($\sim$5%) even at −196 °C. It surpasses most of the other refractory metals in ductility, workability, and weldability. Also, it forms highly stable anodic films on its surface, and therefore at temperatures below 150 °C it is almost completely immune to attack by numerous acids and liquid metals. It forms a stable oxide film, mainly Ta_2O_3, on its surface, although it can easily be contaminated by oxygen at high temperatures during low vacuum annealing [1] or welding.

In addition to the above mentioned favorable properties, pure tantalum and tantalum-based alloys can yield many neutrons under spallation conditions. At an incident proton energy of 1 GeV, for example, more than 18 neutrons are spalled from a tantalum target. This neutron yield is comparable to those of other heavy metals such as tungsten, mercury, and lead [8]. Tantalum and tantalum–tungsten alloys therefore are candidate materials for a spallation neutron source target or target cladding material [4–8]. Since the solid target and its cladding are part of the target structure where its mechanical integrity must be maintained during service, it is important to prevent radiation-induced embrittlement leading to a reduction in its service life.

* Corresponding author.
E-mail address: byunts@ornl.gov (T.S. Byun).

0022-3115/$ - see front matter Published by Elsevier B.V.
doi:10.1016/j.jnucmat.2008.02.034

To provide basic mechanical properties for predicting the integrity of tantalum and tantalum-based alloys in nuclear applications, tensile tests were performed for three pure tantalum metals and two tantalum–tungsten alloys after irradiation in the high flux isotope reactor (HFIR) at Oak Ridge National Laboratory (ORNL) or in the Los Alamos Neutron Scattering Center (LANSCE) facility at Los Alamos National Laboratory (LANL). This paper presents the tensile properties at room temperature and at 250 °C focusing on dose dependence. Further, the strength and ductility data for test materials will be compared to suggest the best material for a spallation target. Discussion will include irradiation effects on true stress parameters and deformation modes.

2. Experimental

Test materials consisted of three pure tantalum metals, ISIS Ta [4], Aesar Ta1, and Aesar Ta2, and two tantalum alloys, Ta–1W and Ta–10W [6,10]. Chemical compositions, heat-treatments, and the initial purity of the pure metals are listed in Table 1. Two types of small tensile specimens, BES/NERI and S-1 types, used. The gage section dimensions of the BES/NERI and S-1 type specimens were 0.25 mm × 1.5 mm × 8 mm and 0.25 mm × 1.2 mm × 5 mm, respectively [6,9]. All machining and mechanical polishing operations were completed before the specimens were annealed at 1200 °C for 2 h (BES/NERI type) or 30 min (S-1 type) in vacuum and assembled into irradiation capsules. The BES/NERI specimens of the first four materials were irradiated in the hydraulic tube (HT) facility of HFIR at ORNL [9], and the S-1 specimens of the two alloys were irradiated in the LANSCE accelerator at LANL [6,10]. Only the Ta–1W alloy was irradiated in both irradiation experiments.

The HT facility of HFIR permits small aluminum rabbit capsules to be shuttled in and out of the reactor core on demand in a stream of coolant water while the reactor is at power. Gamma heat generated in the rabbit is carried away by coolant flow. The target irradiation temperature for the specimens was <100 °C and was obtained by irradiating the specimens in direct contact with the flowing coolant water using rabbits with many perforations through their walls. The temperature of the specimens was estimated to be in the range 60–100 °C. The specimens were irradiated to fast neutron fluences of 1.1×10^{21}, 1.1×10^{22}, 1.1×10^{23}, 1.1×10^{24}, and 4.2×10^{24} n m^{-2}, $E > 0.1$ MeV, corresponding to doses of 0.00004, 0.0004, 0.004, 0.04, and 0.14 dpa, respectively [9].

In the LANSCE facility, specimens were stacked in sealed stainless steel envelopes and irradiated in arrays of horizontal stainless steel tubes through which cooling water flowed. The S-1 tantalum–tungsten alloy tensile specimens were irradiated at different positions with respect to the beam to obtain different exposure levels. The quasi-continuous proton beam had an energy of 800 MeV and an average current of 1 mA. Accumulated on-line exposure period was 3614 h. Dosimetry using metallic foils showed that proton and neutron fluences ranged from 8.3×10^{24} to 3.6×10^{25} p m^{-2} and from 2.9×10^{24} to 1.1×10^{25} n m^{-2}, respectively [10]. A simplified calculation gave the displacement-per-atom (dpa) doses ranging from 0.7 to 7.5 dpa and from 0.7 to 25.2 dpa, for Ta–1W and Ta–10W specimens, respectively [6]. Irradiation temperatures for tantalum alloy specimens were in a range 50–160 °C, depending on the position of the specimens [6,10].

In tensile testing, load is applied to the specimen through its shoulder using cradle-type specimen jigs [9,10]. Tensile tests were conducted in air at room temperature or at 250 °C in screw-driven machines at a crosshead speed of 0.005 mm s^{-1}, corresponding to nominal strain rates of 0.6 and 1.0×10^{-3} s^{-1}, respectively, for BES/NERI specimens and S-1 specimens. Engineering stresses were calculated as the loads divided by the initial cross-sectional area measured before irradiation. 0.2% offset yield strength was obtained when the curve did not show a sharp yield point. The peak strength at yield (yield strength: YS) was also selected as ultimate tensile strength (UTS) when the specimen exhibited a yield drop but did not experience any work-hardening after the yield drop. Also, it was noted that the fracture point on tensile curve was not evident in many pure tantalum specimens. In such cases, fracture strength was determined at the point where the slope of tensile curve was about −500 N/mm, which is comparable to or steeper than the slopes of yield drops observed in this study.

Table 1
Chemical composition, specimen type, heat treatment, and irradiation conditions of test materials

Case #	Material	Purity or tungsten content, wt/%	Specimen type	Annealing time at 1200 °C (final anneal)	Oxygen content (after anneal), wppm	Irradiation facility (radiation)	Dose range, dpa	Irradiation temp., °C
1	Aesar Ta1	99.90	BES/NERI[a]	2 h	224	HFIR (n)	0.00004–0.14	60–100
2	Aesar Ta2	99.95	BES/NERI	2 h	226	HFIR (n)	0.00004–0.14	60–100
3	ISIS Ta	99.95	BES/NERI	2 h	496	HFIR (n)	0.00004–0.14	60–100
4	Ta–1W	1.2%W	BES/NERI	2 h	443	HFIR (n)	0.00004–0.14	60–100
5	Ta–1W	1.2%W	S-1	30 min	443	LANSCE (n < p)	0.7–7.5	50–160
6	Ta–10W	9.3%W	S-1	30 min	327	LANSCE (n < p)	0.7–25.2	50–160

HFIR (n): high flux isotope reactor (irradiation by fast neutron); LANSCE (n < p): Los Alamos Neutron Scattering Center (irradiation by 800 MeV protons + spallation neutrons); (n < p): proton flux was higher than neutron flux.
[a] Basic Energy Science/Nuclear Energy Research Initiative Programs.

3. Results and discussion

3.1. Tensile curves for pure tantalum metals

The engineering stress–strain curves for neutron-irradiated pure tantalum metals are presented in Figs. 1–3. Pure tantalum metals underwent progressive irradiation hardening and loss of ductility with increasing dose. At room temperature the yield and ultimate tensile strengths increased rapidly with dose. Yield stress increased to about 600 MPa after irradiation to 0.14 dpa, 2.5 times higher than those of unirradiated materials ~240 MPa. A yield phenomenon, or a load drop from the upper yield point, was often observed in tantalum metals [1,6]. As seen in Fig. 1, the yield drop was profound in the Aesar materials at low doses. Stress drops from the upper yield points were measured at ~40 MPa for Aesar Ta1 (and for Ta–1W alloy). The yield drop was less evident in the ISIS Ta before irradiation or at the lowest dose of 0.00004 dpa, Fig. 2. In the dose range 0.0004–0.04 dpa, the engineering stress–strain curves were nearly flat over a strain range after yield drop.

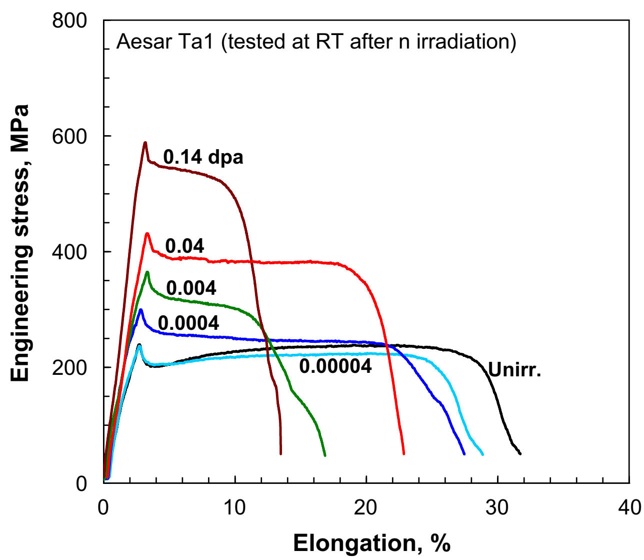

Fig. 1. Engineering stress–strain curves for Aesar Ta1 at room temperature after neutron irradiation.

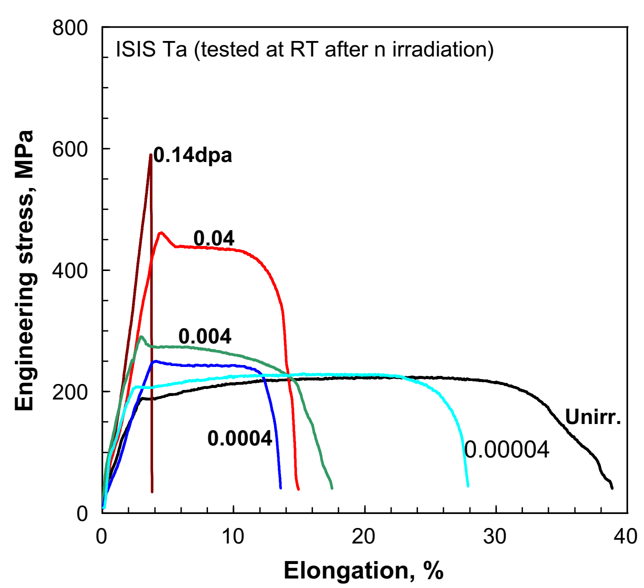

Fig. 2. Engineering stress–strain curves for ISIS Ta at room temperature after neutron irradiation.

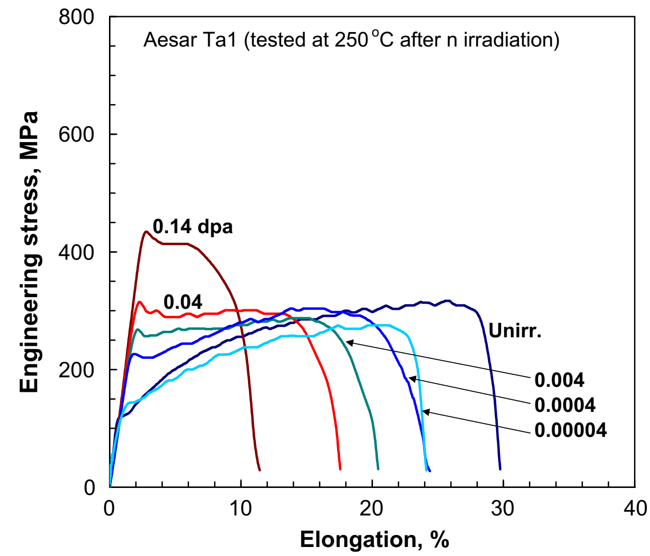

Fig. 3. Engineering stress–strain curves for Aesar Ta1 at 250 °C after neutron irradiation.

Although the ductility of pure tantalum metals before irradiation was extraordinarily high for refractory metals, it decreased rapidly with dose. The loss of uniform ductility was particularly rapid in all test materials; which resulted in an early onset of necking after irradiation to a dose of 0.0004 dpa or higher. While the other metals retained significant necking ductility (7–10%) even after prompt necking at yield occurred, the ISIS Ta experienced embrittlement at 0.14 dpa. Except for this embrittled case, however, the tensile load, or the engineering stress in tensile curve, did not suddenly drop to zero. Shear straining dominated the unstable deformation and failure process, and the specimen remained intact until the load decreased to nearly zero.

Temperature effects in engineering stress–strain curves, which can be shown by comparing Figs. 1 and 3, appeared in two aspects: reduction of strength at all doses and increase of work-hardening at early deformation at 0 dpa and low doses. The yield stress of the Aesar Ta1 material before irradiation was about 130 MPa, and the yield stress more than tripled to 450 MPa at 0.14 dpa. In metallic materials high work-hardening rate usually induces a higher ductility. At 250 °C, however, the increased work-hardening rate at low doses in the Aesar Ta1 was not accompanied by an increase in ductility.

3.2. Tensile curves for tantalum–tungsten alloys

Figs. 4 and 5 present the room temperature tensile curves of Ta–1W alloy after irradiations with neutrons and with mixture of neutrons and protons, respectively. The strength of this material is 30–50% higher than those of the pure metals. Again, a gradual increase of strength and decrease of ductility with dose are found in Fig. 4. After this gradual increase, strength became almost saturated at higher doses, Fig. 5. The tensile curves in Fig. 5, irrespective of dose, displayed an absolute increase in yield stress of about 360 MPa, corresponding to a 100% increase from the yield stress of unirradiated material [6]. Also, the unirradiated Ta–1W specimen showed a yield drop of about 40 MPa. This amount of yield drop was retained after irradiation. However, above 0.004 dpa the yield drops led immediately to necking and negative work-hardening slopes. Note that in such cases the yield stress and ultimate tensile strength for the specimens are almost indistinguishable because of the prompt plastic instability at or near yield.

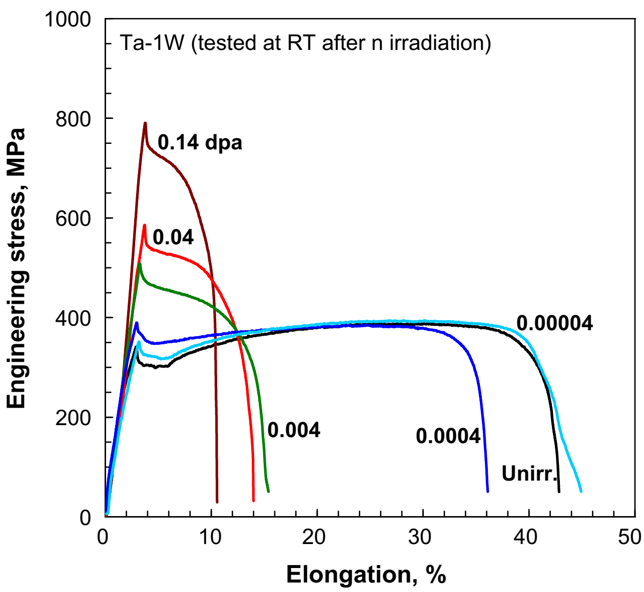

Fig. 4. Engineering stress–strain curves for Ta–1W at room temperature after neutron irradiation.

In the Ta–1W alloy, about 40% total elongation was measured before irradiation, which is ~20% higher than those of pure metals. In the Ta–1W alloy the decrease in uniform and total elongation occurred rather suddenly between 0.0004 and 0.004 dpa, Fig. 4. In Fig. 5, however, no specimen showed brittle fracture at doses up to 7.5 dpa. Although the uniform elongation after 0.004 dpa was negligible, this alloy displayed substantial necking ductility, resulting in at least 7% total elongation, at higher doses up to 7.5 dpa.

The tensile curves for the Ta–1W alloy at 250 °C are presented in Fig. 6. For the Ta–1W alloy before irradiation and after irradiation to 0.004 dpa, lower total elongations were measured at 250 °C than at room temperature. At higher doses, the total elongations measured after prompt necking at yield were in the similar range 7–10%. Temperature effects on other tensile properties of Ta–1W alloy are similar to those of pure metals: strength is 20–40% lower and the work-hardening rate is higher at 250 °C at early deformation stage at zero and low doses.

In Fig. 7, the strength of Ta–10W is much higher compared to those of the Ta–1W alloy or pure metals. Its yield stress before irradiation, 840–880 MPa, is about 3.7 and 2.6 times higher when compared to the pure tantalum metals

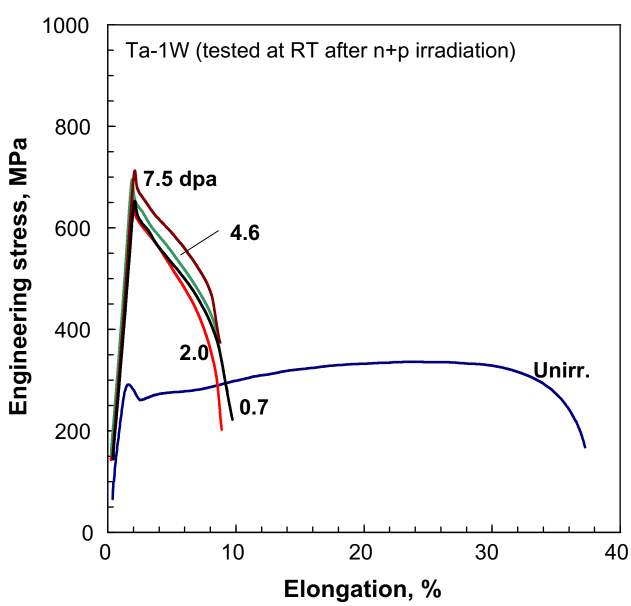

Fig. 5. Engineering stress–strain curves for Ta–1W at room temperature after neutron plus proton irradiation.

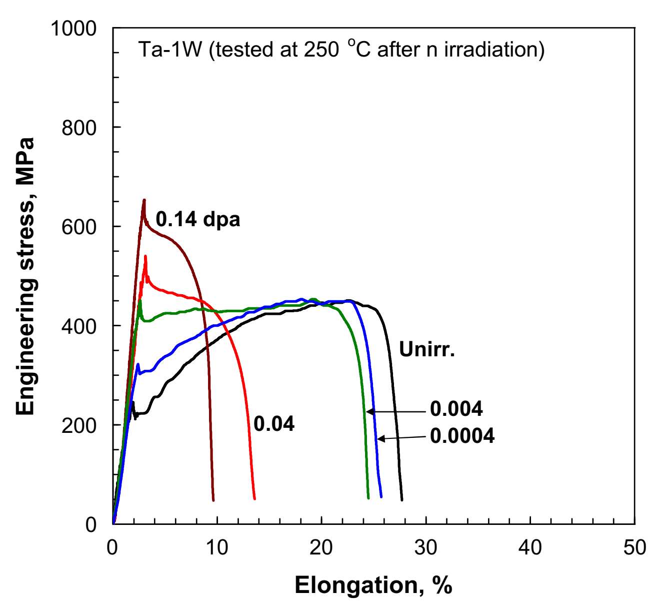

Fig. 6. Engineering stress–strain curves for Ta–1W at 250 °C after neutron irradiation.

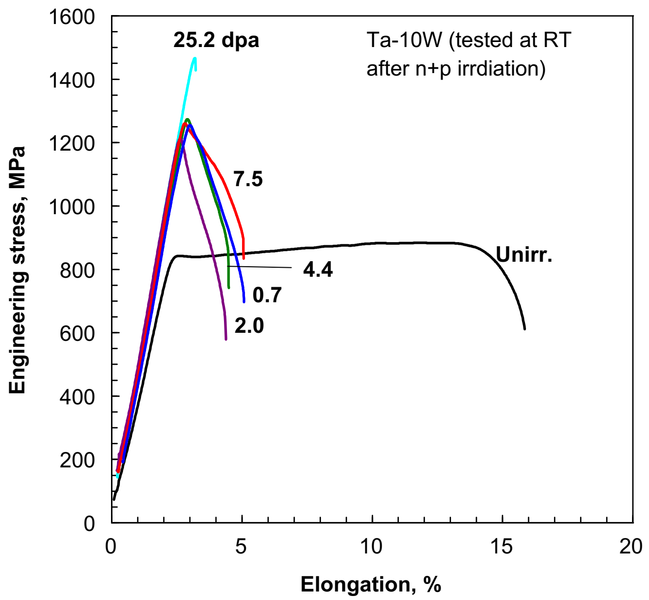

Fig. 7. Engineering stress–strain curves for Ta–10W at room temperature after neutron plus proton irradiation.

and the Ta–1W alloy, respectively [6]. The unirradiated Ta–10W alloy had a yield perturbation with barely detectable load drop and shallow but positive work-hardening. All Ta–10W specimens irradiated under spallation conditions (n plus p irradiation) experienced prompt necking at yield since irradiation doses for those specimens were high (⩾0.7 dpa). Irradiation to doses up to 7.5 dpa induced about 45% increase in yield stress and prompt necking at yield. The total elongations, which consisted of mostly necking ductility, were about 3%. At the highest dose of 25.2 dpa, the engineering stress of the Ta–10W alloy reached 1480 MPa, about 1.7 times the yield stress of the unirradiated material, and then the specimen broke with very little plastic strain.

3.3. Comparison of engineering tensile data

The dose dependence of engineering tensile data, yield stress, ultimate tensile strength, uniform elongation, and total elongation, for all test materials are assembled in Figs. 8–11. In neutron-irradiated pure tantalum metals and the Ta–1W alloy, the dose dependencies of yield stress and tensile strength are similar, as seen in Figs. 8 and 9. For both Aesar Ta1 and Ta–1W alloy, the comparison of the strength data at different temperatures indicates that the change of test temperature does not significantly alter the dose dependences. If combining the strength data for Ta–1W alloy after neutron irradiation and neutron plus proton irradiation, both sets of data seem to follow the common trend line, except for the discontinuity at 0.14 dpa. Also, although no strength data were measured for irradiated Ta–10W alloy below 0.7 dpa, the slope formed by connecting the data at 0 dpa and the data group in the dose range 0.7–7.5 dpa is similar to those for other cases.

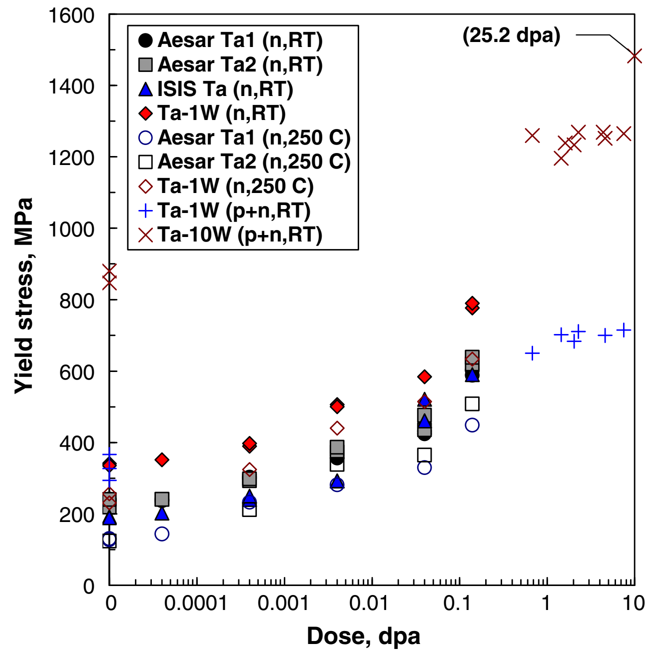

Fig. 8. Dose dependence of yield strength.

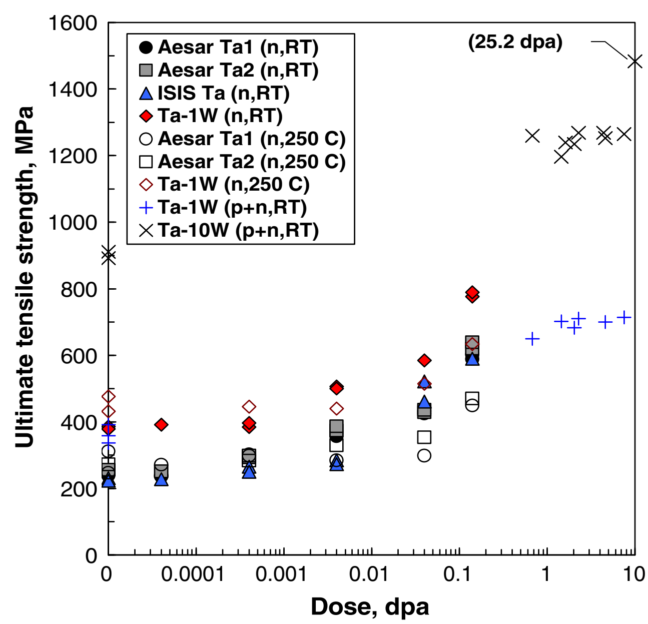

Fig. 9. Dose dependence of ultimate tensile strength.

Ductility data are compared in Figs. 10 and 11. At room temperature all pure tantalum metals displayed almost zero uniform elongation at 0.0004 dpa and no material had measurable uniform ductility above 0.004 dpa. Ductility loss was slower at 250 °C; the Aesar Ta2 retained less than 4% uniform elongation at 0.14 dpa. Total elongation decreased with irradiation dose; however, the test materials retained at least 3% total elongation over test dose range, except for the two brittle failure cases, ISIS Ta at 0.14 dpa and Ta–10W at 25 dpa.

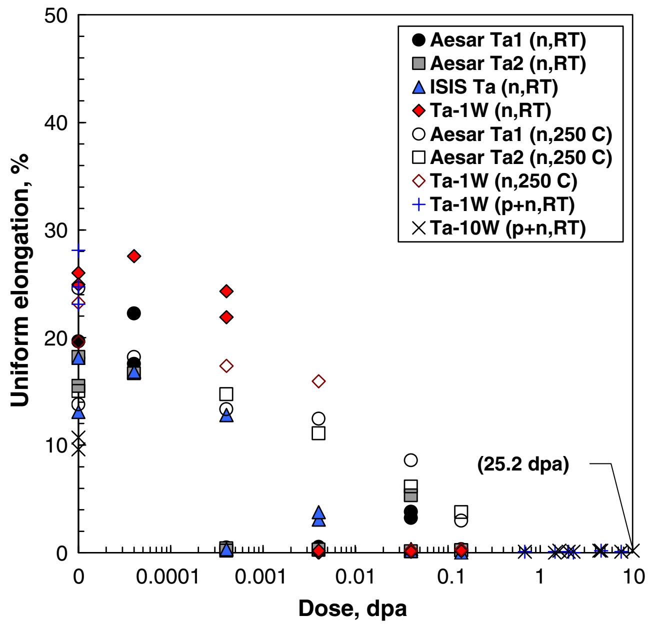

Fig. 10. Dose dependence of uniform elongation.

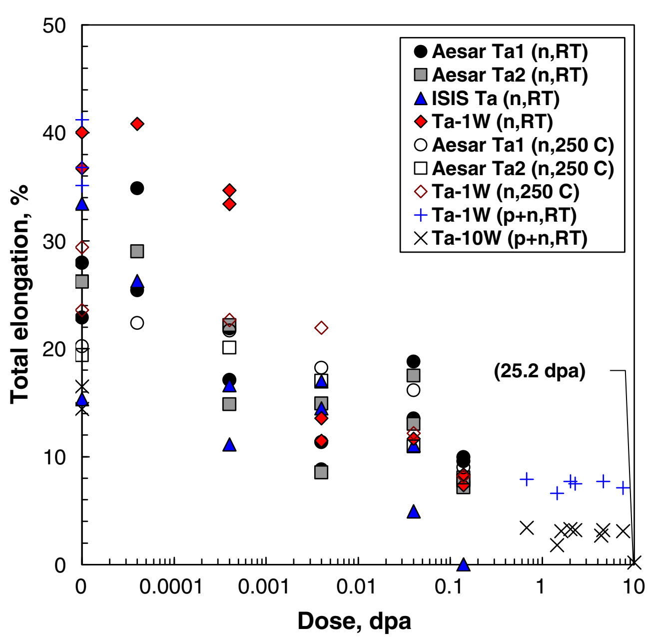

Fig. 11. Dose dependence of total elongation.

The brittle failure of ISIS Ta at 0.14 dpa was premature when compared to other test materials, Aesar Ta1 and Aesar Ta2, and even when compared to the same material irradiated in a different facility. Chen and Ullmaier [4,5] tested the material at the same temperatures, room temperature and 250 °C, after irradiation in spallation condition up to 11 dpa. Their results showed that, although the tensile behavior of the ISIS Ta before irradiation was similar to the present result, ductility loss by irradiation was much lower. At the highest dose, 11 dpa, the material displayed significant uniform elongations (>5%) at room temperature and more than 10% total elongations at room temperature and 250 °C. Although the strength level in their tests was similar to those obtained in the present work, the rate of increase in yield stress with dose was significantly lower.

It is known that tantalum absorbs trace quantities of interstitial elements, such as oxygen and nitrogen, at elevated and high temperatures [1]. The discrepancy between the present elongation data and the Chen and Ullmaier's data is believed to be because of oxygen contamination during specimen preparation or annealing in the present work, and therefore, elemental analysis on oxygen and nitrogen contents using LECO TC600 system was performed for unirradiated specimens. The result showed that the ISIS Ta contained ~500 ppm oxygen and Aesar Ta1 and Ta2 ~220 ppm oxygen, Table 1. These contents are about 10 times higher than those measured before heat treatment. Nitrogen contents were much lower: ~5% of the oxygen content. It is believed that a synergistic effect of high oxygen content and radiation effect has reduced the fracture strength of ISIS Ta. It is also known that such interstitial elements in tantalum increase hardness [1]. It is therefore believed that the three pure tantalum metals have higher strength than those without oxygen contamination. It should be also considered that the specimens were exposed to water coolant in HFIR irradiation while the specimens were sealed in stainless steel envelopes in LANSCE irradiation. Even if the irradiation temperature at HFIR was low (~80 °C), it might be possible that the contact with water allowed the specimens to take additional oxygen content during irradiation and resulted in higher irradiation hardening in the HFIR irradiated specimens.

3.4. Deformation mode maps and temperature effect

A ductile specimen under uniaxial tensile load experiences elastic, uniform, and unstable deformation and fracture, and irradiation will change the deformation and fracture behavior of the material. A macroscopic deformation mode map in true stress–dose space can be used for predicting the performance of a material in irradiation environments. Building such a deformation mode map requires true stress data such as yield stress, plastic instability stress (PIS), and fracture stress (FS) to define boundaries between the deformation modes [13]. The YS and PIS values are directly obtained from the engineering tensile data while the FS value is calculated from engineering fracture stress data through a model described elsewhere [11–13]. The plastic instability stress is the true stress version of ultimate tensile strength. The calculation of FS is based on a linear strain-hardening model for necking deformation, where the strain-hardening rate remains unchanged during instable deformation and is approximately the same as the plastic instability stress [13,14].

Figs. 12 and 13 present deformation mode maps at room temperature for pure tantalum metals after neutron irradiation and the Ta–1W alloy after neutron or neutron plus proton irradiation, respectively. Both deformation maps

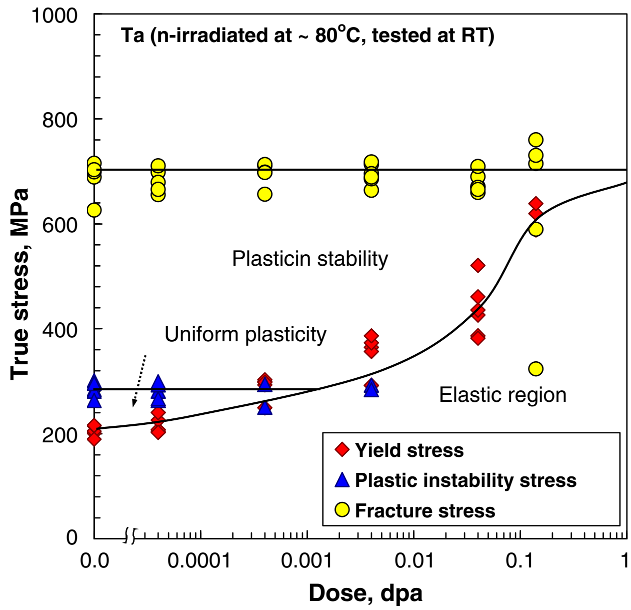

Fig. 12. Macroscopic deformation mode map for pure tantalum metals.

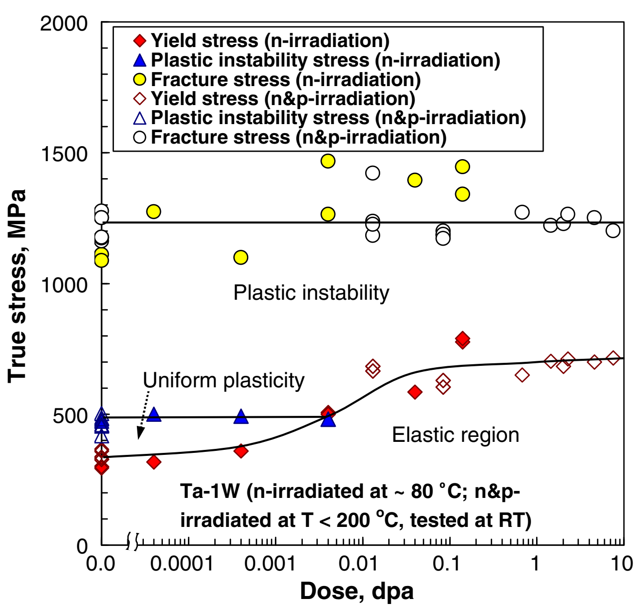

Fig. 13. Macroscopic deformation mode map for Ta–1W alloy.

indicate that PIS and FS are nearly independent of dose, while YS is strongly dose dependent. This dose independence of PIS and FS was observed in many other materials [11–14]. At room temperature the PIS values of pure tantalum metals were in the range 270–300 MPa, and those of the Ta–1W alloy are in the range 450–490 MPa. The average FS values were evaluated to be 600–800 MPa for pure metals and 1200–1300 MPa for the Ta–1W alloy. Also note that much higher PIS and FS values, ~990 MPa and ~2350 MPa, respectively, were found for the Ta–10W alloy. For all test materials, the ratio of FS to PIS was about two or higher.

FS will decrease with dose if the material is affected by any radiation-induced embrittlement mechanism [13]. During embrittlement, the material will experience brittle failure when the YS line meets with the FS line. This actually occurred in the ISIS Ta at 0.14 dpa and Ta–10W at 25.2 dpa. A notable fact found in Fig. 13 for Ta–1W is that the YS line is far below the FS line at the highest dose 7.5 dpa. This indicates that the Ta–1W alloy may not experience embrittlement any time soon, or until the irradiation dose reaches a 20–30 dpa. This prediction is an evidence that Ta–1W can be a good candidate material for spallation target applications, in addition to the best combination of strength and ductility as mentioned above.

Above the yield stress line, the plastic deformation region consists of two different regions: stable (or uniform) deformation and unstable (or necking) deformation regions. Comparing the sizes of regions of deformation modes, the mode maps for the tantalum materials are characterized by a relatively large plastic instability region and a narrow uniform deformation region, which should be due to large necking ductility and relatively low strain-hardening rate (this usually results in low uniform ductility), respectively. This feature is common for many body-centered cubic and hexagonal close packed metals [13].

The effect of temperature on the uniform deformation region is presented in Figs. 14 and 15, for pure metals (Aesar Ta1 and Ta2) and Ta–1W alloy, respectively. Increasing test temperature from room temperature to 250 °C enlarged the uniform deformation region many folds in pure tantalum and about two folds in Ta–1W alloy. This delayed the onset of necking at yield, where YS reaches PIS, to a higher dose of ~0.1 dpa. It is also noted that this delay is attributed to the decrease in YS and increase in PIS by increasing test temperature.

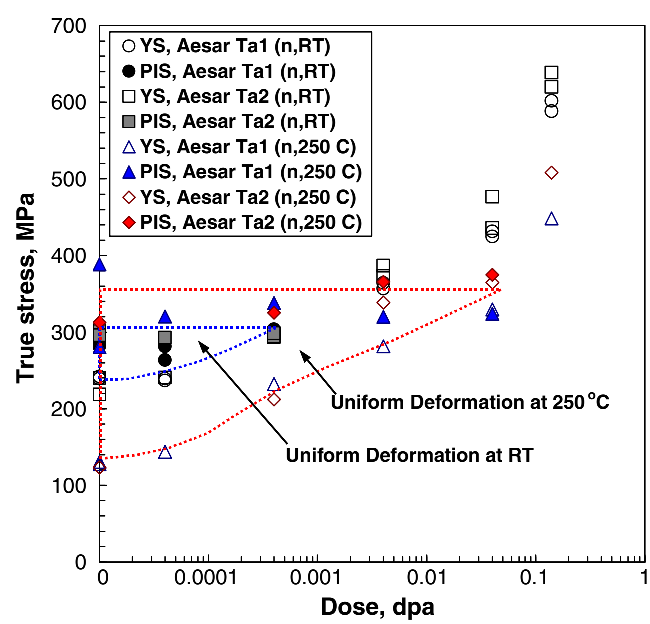

Fig. 14. Temperature effect on uniform deformation region in Aesar tantalum.

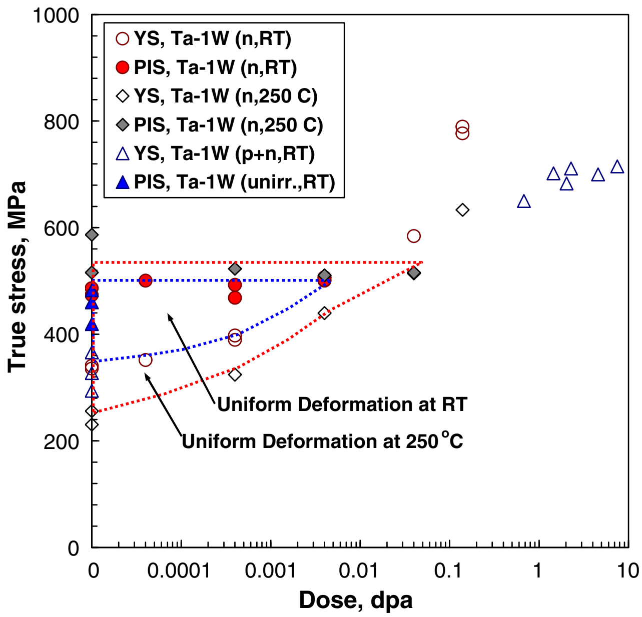

Fig. 15. Temperature effect on uniform deformation region in Ta–1W alloy.

4. Conclusions

Dose dependence of tensile properties was investigated for pure tantalum metals and tantalum–tungsten alloys after low temperature neutron or neutron plus proton irradiation. Conclusions derived from tensile test and analysis results are given as follows:

(1) The pure tantalum metals and tantalum–tungsten alloys display high ductility, up to 40% total elongation, before irradiation. The low temperature irradiation resulted in a large increase in yield strength and decrease in ductility after irradiation to 0.14 dpa. Significant yield drop occurred in most of irradiated and unirradiated specimens.
(2) Among the test materials, the Ta–1W alloy showed the best combination of strength and ductility, which indicates that the alloy can be a primary candidate for target or target cladding material. Deformation mode map indicates that the Ta–1W alloy may not be embrittled until radiation dose reaches a few tens of dpa.
(3) Plastic instability stress was nearly independent of dose; however, it increased with test temperature. Uniform deformation region was larger at 250 °C than at room temperature, which delayed the onset of necking at yield to a higher dose ~0.1 dpa.
(4) True fracture stress was nearly dose independent and at least two times higher than the plastic instability stress before embrittlement occurs.
(5) The rate of decrease in uniform elongation and increase in yield stress with increasing dose observed in the pure tantalum alloys is much higher than previously reported by Chen et al. [5]. This difference is believed to be caused by the high oxygen content of these pure tantalum materials which was picked up during annealing before irradiation.

Acknowledgements

This research was sponsored by US Department of Energy, Office of Fusion Energy Sciences, under Contract DE-AC05-00OR22725 with UT-Battelle, LLC. The authors would like to express special thanks to Drs J.T. Busby and M. Li for their technical reviews and thoughtful comments.

References

[1] T.E. Tietz, J.W. Wilson, Behavior and Properties of Refractory Metals, Stanford University, Stanford, California, 1965.
[2] S.N. Mathaudhu, K.T. Hartwig, Mater. Sci. Eng. A 426 (2006) 128.
[3] Y. Li, W. Cai, E.J. Lavernia, F.A. Mohamed, in: TMS Annual Meeting, Anaheim, California, February 4–8, 1996.
[4] J. Chen, H. Ullmaier, T. Floßdorf, W. Kühnlein, R. Duwe, F. Carsughi, T. Broome, J. Nucl. Mater. 298 (2001) 248.
[5] J. Chen, P. Jung, M. Rödig, H. Ullmaier, G.S. Bauer, J. Nucl. Mater. 343 (2005) 227.
[6] T.S. Byun, K. FarrellFourth International Topical Meeting on Nuclear Applications of Accelerator Technology (AccApp-2000), American Nuclear Society, Washington, DC, 2000, p. 270.
[7] C. Villagrasa-Roussel, C.H.M. Broeders, A.Y. Konobeyev, Kerntechnik 71 (2006) 3.
[8] N. Watanabe, Rep. Prog. Phys. 66 (2003) 339.
[9] K. Farrell, T.S. Byun, N. Hashimoto, J. Nucl. Mater. 335 (2004)]471.
[10] K. Farrell, T.S. Byun, Tensile Properties of Candidate SNS Target and Container Materials after Proton and Neutron Irradiation in the LANSCE Accelerator, SNS/TSR-193 (SNS-101060100-TR0002-R00), Oak Ridge National Laboratory, 2001.
[11] T.S. Byun, K. Farrell, Acta Mater. 52 (2004) 1597.
[12] T.S. Byun, N. Hashimoto, Nucl. Eng. Technol. 38 (2006) 619.
[13] T.S. Byun, J. Nucl. Mater. 361 (2007) 239.
[14] T.S. Byun, N. Hashimoto, K. Farrell, Acta Mater. 52 (2004) 3889.